# Anisotropic and Long-Range Vortex Interactions in Two-Dimensional Dipolar Bose Gases

B. C. Mulkerin,[1] R. M. W. van Bijnen,[2] D. H. J. O'Dell,[3] A. M. Martin,[1] and N. G. Parker[4]

[1]*School of Physics, University of Melbourne, Victoria 3010, Australia*
[2]*Eindhoven University of Technology, P.O. Box 513, 5600 MB Eindhoven, Netherlands*
[3]*Department of Physics and Astronomy, McMaster University, Hamilton, Ontario L8S 4M1, Canada*
[4]*Joint Quantum Centre Durham-Newcastle, School of Mathematics and Statistics, Newcastle University, Newcastle upon Tyne NE1 7RU, United Kingdom*

(Received 13 July 2013; published 22 October 2013)

We perform a theoretical study into how dipole-dipole interactions modify the properties of superfluid vortices within the context of a two-dimensional atomic Bose gas of co-oriented dipoles. The reduced density at a vortex acts like a giant antidipole, changing the density profile and generating an effective dipolar potential centred at the vortex core whose most slowly decaying terms go as $1/\rho^2$ and $\ln(\rho)/\rho^3$. These effects modify the vortex-vortex interaction which, in particular, becomes anisotropic for dipoles polarized in the plane. Striking modifications to vortex-vortex dynamics are demonstrated, i.e., anisotropic corotation dynamics and the suppression of vortex annihilation.

DOI: 10.1103/PhysRevLett.111.170402 PACS numbers: 05.30.Jp, 03.75.Hh, 03.75.Lm, 47.37.+q

Ferrohydrodynamics (FHD) describes the motion of fluids made of particles with magnetic (or electric) dipoles [1,2]. The interparticle dipole-dipole interactions (DDIs) are long range and anisotropic, giving rise to behavior such as magnetostriction and electrostriction, geometric pattern formation and surface ripple instabilities [3]. The distinctive properties of ferrofluids are exploited in applications from tribology to information display and medicine [1]. Recently, quantum ferrofluids have been realized through Bose-Einstein condensates (BECs) of atoms with large magnetic dipole moments [4] such as $^{52}$Cr [5,6], $^{164}$Dy [7], and $^{168}$Er [8]. Signatures of FHD have been observed in these gases, including magnetostriction [9] and $d$-wave collapse [10]. Pattern formation [11–13], linked to roton-like excitations [13–15], has been predicted but not yet seen. Superfluidity of semiconductor microcavity polaritons, which are inherently dipolar, has also recently been demonstrated [16].

In this Letter we consider the interplay between DDIs and vortices in a BEC. Vortices form the "sinews and muscles" of fluids [17,18] and drive phenomena such as mixing processes, sunspots, tornadoes, and synoptic scale weather phenomena [19]. In a superfluid BEC the vortices have a core of well-defined size and quantized vorticity. Single vortices, vortex rings, pairs, lattices, and turbulent states can be controllably generated [20] and imaged in real time [21]. In quasi-2D geometries, the paradigm of point vortices [22,23] can be realized. 2D Bose gases also provide a route to the Berezinsky-Kosterlitz-Thouless (BKT) transition [24], the thermal unbinding of vortex-antivortex pairs (VA).

Previous theoretical studies of a vortex in a trapped 3D dipolar BEC found density ripples about the core [25–27] and an elliptical core [25]. Here we consider the quasi-2D case and focus on the effective long-range and anisotropic potentials that are generated between vortices by DDIs. We demonstrate the striking implications of these potentials on the motion of pairs of vortices. Our results provide insight into the role of DDIs in large-scale superfluid phenonema, such as the vortex lattice phases [28], the BKT transition, and quantum turbulence.

When the dipoles are aligned by an external field, the DDIs are described by

$$U_{\rm dd}(\mathbf{r}-\mathbf{r}') = \frac{C_{\rm dd}}{4\pi}\frac{1-3\cos^2\theta}{|\mathbf{r}-\mathbf{r}'|^3}, \tag{1}$$

where $\theta$ is the angle between the polarization direction and the interparticle vector $\mathbf{r}-\mathbf{r}'$. For magnetic dipoles with moment $d$, $C_{\rm dd} = \mu_0 d^2$, where $\mu_0$ is the permeability of free space. The strongly dipolar $^{164}$Dy BEC [7] has $d = 10\mu_B$ (Bohr magnetons). The same interaction arises between polar molecules, which can possess huge electric dipole moments and have been cooled close to degeneracy [29]. A BEC with DDIs is described by the dipolar Gross-Pitaevskii equation (DGPE) [4], in which the DDIs are incorporated via Eq. (1), and the isotropic van der Waals interactions (vdWIs) via a local pseudopotential $U_{\rm vdW}(\mathbf{r}-\mathbf{r}') = g_{\rm 3D}\delta(\mathbf{r}-\mathbf{r}')$ [30]. The relative strength of the DDIs is parametrized via the ratio $\varepsilon_{\rm dd} = C_{\rm dd}/3g_{\rm 3D}$ [4]. This parameter has a natural value $\varepsilon_{\rm dd} \lesssim 1$. However, the ability to tune $g_{\rm 3D}$ between $-\infty$ and $+\infty$ via Feshbach resonance has enabled the realization of a purely dipolar gas ($\varepsilon_{\rm dd} = \infty$) [31]. Furthermore, it is predicted that $C_{\rm dd}$ can be reduced below its natural, positive value, including to negative values, by external field rotation [32]. As such, a large parameter space $-\infty < \varepsilon_{\rm dd} < \infty$, with positive or negative $g_{\rm 3D}$ and $C_{\rm dd}$, is possible.

We consider bosonic dipoles of mass $m$, free in the transverse ($\boldsymbol{\rho}$) plane and with harmonic trapping in the axial ($z$) direction. The axial trap frequency $\omega_z$ is sufficiently

 

strong that the BEC is frozen into the axial ground harmonic state of width $l_z = \sqrt{\hbar/m\omega_z}$ [33]. The polarization axis is at angle $\alpha$ to the $z$ axis in the $xz$ plane. Integrating over $z$ gives the effective 2D DGPE for the 2D wave function $\psi(\boldsymbol{\rho}, t)$ [34],

$$i\hbar\frac{\partial\psi}{\partial t} = \left[-\frac{\hbar^2}{2m}\nabla^2 + g|\psi|^2 + \Phi - \mu\right]\psi, \qquad (2)$$

with chemical potential $\mu$. The mean-field potentials $gn(\boldsymbol{\rho}, t)$ and $\Phi(\boldsymbol{\rho},t) = \int U_{\rm dd}^{\rm 2D}(\boldsymbol{\rho}-\boldsymbol{\rho}')n(\boldsymbol{\rho}',t)d\boldsymbol{\rho}'$ account for the vdWIs and DDIs, respectively, where $n = |\psi|^2$ is the 2D particle density, $U_{\rm dd}^{\rm 2D}$ is the effective 2D DDI potential, and $g = g_{\rm 3D}/\sqrt{2\pi}l_z$. While an explicit expression for $U_{\rm dd}^{\rm 2D}(\boldsymbol{\rho})$ exists [35], it is convenient to work in Fourier space and use the convolution theorem $\Phi(\boldsymbol{\rho}, t) = \mathcal{F}^{-1}[\tilde{U}_{\rm dd}^{\rm 2D}(\mathbf{k})\tilde{n}(\mathbf{k}, t)]$ [34,36]. The Fourier transform of $U_{\rm dd}^{\rm 2D}(\boldsymbol{\rho})$ is $\tilde{U}_{\rm dd}^{\rm 2D}(\mathbf{q}) = (4\pi g_{\rm dd}/3)[F_{\|}(\mathbf{q})\sin^2\alpha + F_{\perp}(\mathbf{q})\cos^2\alpha]$, with $\mathbf{q} = \mathbf{k}l_z/\sqrt{2}$, $F_{\|}(\mathbf{q}) = -1 + 3\sqrt{\pi}(q_x^2/q)e^{q^2}\mathrm{erfc}(q)$, $F_{\perp}(\mathbf{q}) = 2 - 3\sqrt{\pi}qe^{q^2}\mathrm{erfc}(q)$, and $g_{\rm dd} = C_{\rm dd}/3\sqrt{2\pi}l_z$. It follows that $\varepsilon_{\rm dd} = g_{\rm dd}/g$.

A homogeneous 2D dipolar gas of density $n_0$ has uniform dipolar potential $\Phi_0 = n_0 g_{\rm dd}(3\cos^2\alpha - 1)$ and chemical potential $\mu_0 = n_0(g + g_{\rm dd}[3\cos^2\alpha - 1])$ [33–35]. At the "magic angle" $\alpha_0 = \arccos(1/\sqrt{3}) \approx 54.7°$, $\Phi_0$ is zero. For $\alpha < \alpha_0$, $\Phi_0$ is net repulsive (attractive) for $g_{\rm dd} > 0$ ($< 0$), while for $\alpha > \alpha_0$ it is net attractive (repulsive) for $g_{\rm dd} > 0$ ($< 0$). The system suffers two key instabilities. The phonon instability (PI), familiar from conventional BECs [30], is associated with unstable growth of zero momentum modes. It arises when the net local interactions become attractive, i.e., when $\mu_0 < 0$. In terms of $\varepsilon_{\rm dd}$, it follows that the PI arises for $\varepsilon_{\rm dd} < [1 - 3\cos^2\alpha]^{-1}$ when $g > 0$ or $\varepsilon_{\rm dd} > [1 - 3\cos^2\alpha]^{-1}$ when $g < 0$ [4,15,36–38].

DDIs can induce a roton dip at finite momentum in the excitation spectrum [14,15,27]. When this softens to zero energy, the roton instability (RI) arises in finite momentum modes. A collapse ensues via density ripples aligned either along the polarization axis (for $C_{\rm dd} > 0$) or perpendicular to it (for $C_{\rm dd} < 0$) due to the preferred alignment of dipoles end to end or side by side, respectively [11]. Close to the RI stable density ripples arise when the roton mode mixes into the ground state [25,27]. Typically, the RI is induced by the attractive part of the DDI. An exception arises for the 2D gas with dipoles polarized along $z$; the attractive part of the DDI lies out of the plane where the particles cannot access it [36] but a roton can be induced via attractive local interactions [39]. For dipoles polarized in the plane, the particles can access the attractive part of the DDI, and the "conventional" dipolar roton is supported.

As a precursor to understanding the vortex-vortex (VV) interaction we first explore single vortex solutions in our 2D homogeneous system (in contrast to the previous analyses in 3D [25,27]). We obtain vortex solutions and dynamics by numerically solving Eq. (2) [40]. Density, energy, and length are scaled in units of $n_0$, $\mu_0$ and the corresponding healing length $\xi_0 = \hbar/\sqrt{m\mu_0}$, respectively. The vortex core size is of the order of $\xi_0$, which diverges as $\mu_0 \to 0$. The 2D approximation is valid for $\sigma = l_z/\xi_0 \lesssim 1$; we choose $\sigma = 0.5$. We consider the representative cases of $\alpha = 0$ (dipoles parallel to the $z$ axis) and $\alpha = \pi/4$ (dipoles tipped partly along $x$ axis).

$\alpha = 0$.—Figure 1(a) shows the vortex density along $x$ and $y$ as a function of $\varepsilon_{\rm dd}$. The dipolar potential, and hence the density profile, are axisymmetric. For $\varepsilon_{\rm dd} = 0$ (left inset) the vortex has the standard axisymmetric core of vanishing density of width $\xi_0$ [30]. For $g > 0$ the system is stable from $\varepsilon_{\rm dd} = -0.5$, the PI threshold, upwards. No RI is observed for $g > 0$, as expected [36]. Meanwhile, for $g < 0$ we only find solutions for $\varepsilon_{\rm dd} \lesssim -1.16$, the RI threshold (red dashed line).

The vortex structure for $\varepsilon_{\rm dd} \neq 0$ is almost identical to the $\varepsilon_{\rm dd} = 0$ case [41], apart from in two regimes. As one approaches $\varepsilon_{\rm dd} = -0.5$ from above, the vortex core becomes increasingly narrow with respect to $\xi_0$ (middle inset), due to the cancellation of explicit contact interactions. Meanwhile, as the RI is approached from below, axisymmetric density ripples appear around the vortex (like in the 3D case [25–27]), decaying with distance and with an amplitude up to $\sim 20\% n_0$ (see third inset). The ripple wavelength is $\approx 4\xi_0$ [42], implying that our treatment is self-consistently 2D because $\sigma = l_z/\xi_0 = 0.5$.

$\alpha = \pi/4$.—The axisymmetry of the dipolar potential and density is lost [Fig. 1(b)]. For $g_{\rm dd} > 0$ ($< 0$) the dipoles lie preferentially along $x$ ($y$). For $g < 0$ we find no stable solutions (down to $\varepsilon_{\rm dd} = -20$) due to the RI. For $g > 0$ we observe the RI, unlike for $\alpha = 0$, since the atoms now feel the attractive part of $U_{\rm dd}$. The RI occurs for $\varepsilon_{\rm dd} \gtrsim 14.9$

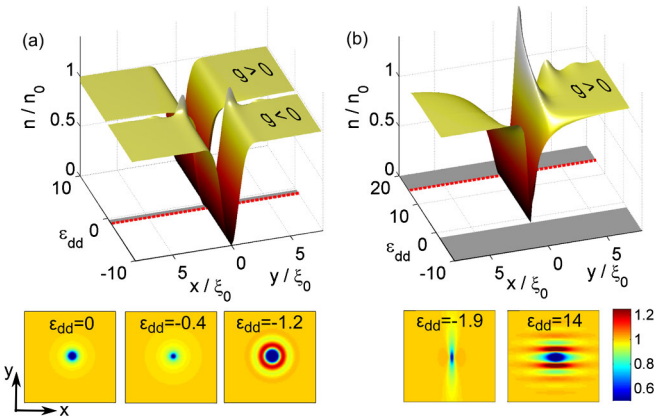


FIG. 1 (color online). Vortex density profiles in the presence of DDIs parametrized by $\varepsilon_{\rm dd} = g_{\rm dd}/g$. The left-hand (right-hand) side of each figure shows the profile along $x$ ($y$). (a) Polarization along $z$ ($\alpha = 0$). Stable density ripples form close to the onset of the RI (dashed red line). (b) For off-axis dipoles ($\alpha = \pi/4$) the vortex becomes highly anisotropic. Insets: Vortex density $n(x, y)$ for examples of $\varepsilon_{\rm dd}$ [area $(40\xi_0)^2$ for each]. Gray bands indicate unstable regimes where no steady state solutions exist, while the labels $g > 0$ and $g < 0$ on the individual solution sheets indicate that they are only stable for the specified value of $g$.

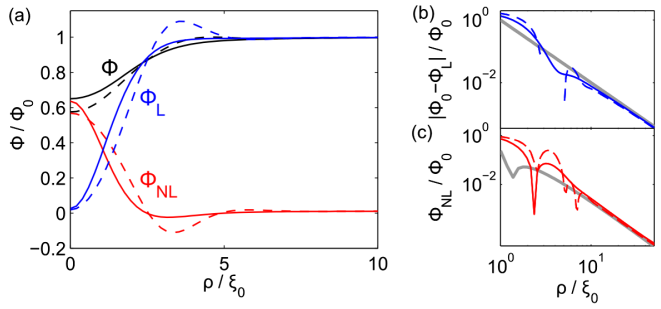


FIG. 2 (color online). (a) The total dipolar potential $\Phi$ (black lines labelled $\Phi$), local component $\Phi_L$ (blue lines labelled $\Phi_L$), and nonlocal component $\Phi_{NL}$ (red lines labelled $\Phi_{NL}$) for a vortex with ripples ($\varepsilon_{dd} = -1.2$, $g < 0$, dashed lines) and without ripples ($\varepsilon_{dd} = 5$, $g > 0$, solid lines). (b) The decay of $\Phi_L/\Phi_0$, compared with $1/\rho'^2$ (gray line). (c) The decay of $\Phi_{NL}/\Phi_0$, compared with $(A\ln\rho' + B)\sigma/\rho'^3$. Parameters are $\alpha = 0$, $\sigma = 0.5$.

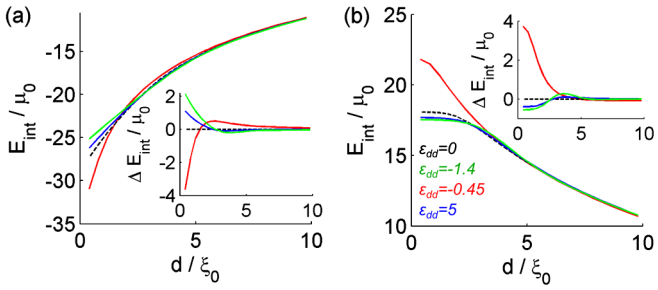


FIG. 3 (color online). Vortex interaction energy $E_{int}$ versus separation for (a) VA and (b) VV pairs with various $\varepsilon_{dd}$ values. Insets: Energy difference from the nondipolar case, $\Delta E_{int} = E_{int}(d, \varepsilon_{dd}) - E_{int}(d, \varepsilon_{dd} = 0)$. Parameters are $\alpha = 0$, $\sigma = 0.5$.

(red dashed line). Below this, stable solutions exist down to the PI threshold $\varepsilon_{dd} = -2$. The vortex core is elongated along $x$ for $\varepsilon_{dd} > 0$, and reverses for $\varepsilon_{dd} < 0$. Close to the RI, density ripples form about the vortex (of large amplitude up to ~40%) aligned along $x$.

We see the same qualitative behavior for all $0 < \alpha < \alpha_0$, albeit with shifted RI and PI thresholds. For cases with $\alpha > \alpha_0$, we see a reversal in the $\varepsilon_{dd}$ dependence, with no solutions for $g > 0$ and ripples polarized along $y$.

From the FHD perspective, the depleted density due to a vortex acts like a lump of "antidipoles" whose charges have been reversed [43]. Let us calculate the mean-field dipolar potential $\Phi(\boldsymbol{\rho})$ generated by such a defect located at $\boldsymbol{\rho} = 0$; we shall see shortly how it modifies the vortex-vortex interaction. For simplicity we consider $\alpha = 0$ and the illustrative cases of $\varepsilon_{dd} = -1.2$ (vortex with ripples, $g < 0$) and 5 (vortex with no ripples, $g > 0$) [Fig. 2(a)]. As $\rho \to \infty$, $\Phi \to \Phi_0 = n_0 g_{dd}(3\cos^2\alpha - 1)$, the homogeneous result, while for $\rho \lesssim 5\xi$, $\Phi$ is dominated by the core structure and ripples (where present). It is insightful to consider $\Phi$ as the sum of a local term $\Phi_L(\boldsymbol{\rho}) = n(\boldsymbol{\rho})g_{dd}(3\cos^2\alpha - 1)$ and a nonlocal term $\Phi_{NL}(\boldsymbol{\rho})$ [33,35,37]. The latter is generated by variations in the density [33,37] and vanishes for a homogeneous system. The generic functional form of $\Phi$ at long range is revealed by assuming the vortex ansatz $n(\rho) = n_0[1 - 1/(1 + \rho'^2)]$, where $\rho' = \rho/\xi_0$ [44,45]. We employ a first-order expansion in $\sigma$ of $\tilde{U}_{dd}^{2D}(\mathbf{k}) = g_{dd}(2 - \sqrt{(9\pi/2)}k\sigma) + O(\sigma^2)$ and the Hankel transform $\tilde{n}(\mathbf{k}) = n_0\delta(k)/k + n_0 K_0(k/\sqrt{2})/2$, where $K_0(k)$ is a modified Bessel function of the second kind [46]. Then, to first order in $\sigma$ and third order in $1/\rho'$,

$$\frac{\Phi(\rho)}{\Phi_0} \sim \left(1 - \frac{1}{\rho'^2}\right) + \left(\frac{A\ln\rho' + B}{\rho'^3}\right)\sigma, \qquad (3)$$

with constants $A = -\sqrt{9\pi/8} \approx -1.88$ and $B = (\ln 2 - 1)A \approx 0.577$. The first term corresponds to the *local* contribution of the vortex dipolar potential [Fig. 2(b), gray line]. It physically arises from the $1/\rho'^2$ decay of vortex density at long range, and is also present for nondipolar vortices (albeit controlled by $g$ and not $g_{dd}$) [47]. The second term describes the *nonlocal* contribution [Fig. 2(c), gray line]. This vanishes in the true 2D limit $\sigma = 0$ since the volume of antidipoles in the core vanishes. Equation (3) agrees with numerical calculations in the limit $\rho' \gg 1$ [Figs. 2(b) and 2(c)]. The dominant scaling of $\Phi_{NL}$ as $\ln\rho'/\rho'^3$, and not $1/\rho'^3$, shows us that the vortex does not strictly behave as a pointlike collection of dipoles at long range. This is due to the slow, power-law recovery of the vortex density to $n_0$. We have checked that exponentially decaying density profiles, e.g., $\tanh^2(\rho')$, do lead to a $1/\rho'^3$ scaling of $\Phi_{NL}$ at long range. For $\alpha \neq 0$, $\Phi$ also varies anisotropically as $\cos^2\theta$ at long range.

We now explore the vortex-vortex interaction through the interaction energy [40]. Figure 3 shows $E_{int}$ for $\alpha = 0$ and [3(a)] vortex-antivortex and [3(b)] vortex-vortex pairs as a function of their separation $d$. For the conventional $\varepsilon_{dd} = 0$ case (dashed line) $E_{int}$ is negative (positive) for VA (VV) pairs due to the cancellation (reinforcement) of velocity fields at large distance. For $d \gtrsim 4\xi_0$, $E_{int}(d) \approx (2\pi q_1 q_2 \hbar^2 n_0/m)\ln(R/d)$, the hydrodynamic (coreless vortex) prediction [30] for system size $R$. For $d \lesssim 4\xi_0$, the cores overlap causing $|E_{int}|$ to flatten off.

When $\varepsilon_{dd} \neq 0$, the logarithmic, hydrodynamic contribution to $E_{int}(d)$ dominates the dipolar contribution for large $d$. Elsewhere, significant deviations to $E_{int}(d)$ arise, particularly at short range $d \lesssim 3\xi_0$. This deviation is most striking for $-0.5 < \varepsilon_{dd} < 0$ ($g > 0$), e.g., $\varepsilon_{dd} = -0.45$ (red lines), for which $|E_{int}|$ increases dramatically as $d$ decreases. This is due to the narrowing of the vortex core (relative to $\xi_0$) as $\varepsilon_{dd} \to -0.5$, reducing the core overlap as $d \to 0$. Outside of this range, for small $d$ ($d \lesssim 3\xi_0$), DDIs reduce $|E_{int}|$. For values of $\varepsilon_{dd}$ that support density ripples, $|E_{int}|$ features a small peak at $d \sim 4\xi$ due to ripple overlap. Further out, $E_{int}$ decays as $1/\rho^2$ towards the $\varepsilon_{dd} = 0$ result. Note that as $|\varepsilon_{dd}|$ is increased, $E_{int}(d)$ tends towards a fixed behavior, independent of the sign of $\varepsilon_{dd}$ (since both cases become dominated by large, positive $g_{dd}$).

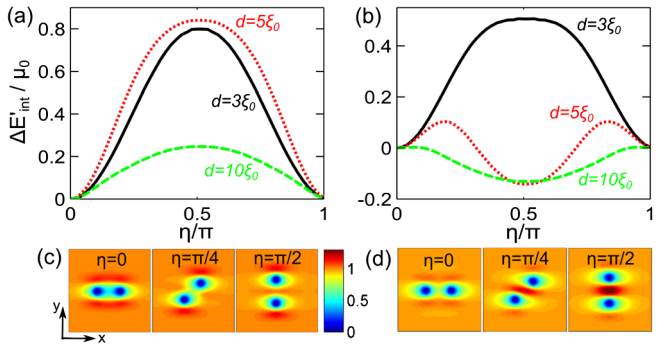


FIG. 4 (color online). Angular dependence of the vortex interaction energy $\Delta E'_{\rm int}(\eta) = E_{\rm int}(\eta) - E_{\rm int}(\eta = 0)$, for (a) VA and (b) VV pairs of differing separation. Parameters are $\alpha = \pi/4$, $\sigma = 0.5$, and $\varepsilon_{\rm dd} = 5$ ($g > 0$). Example (c) VA and (d) VV pair density profiles for $d = 5\xi_0$ [area $(20\xi_0)^2$ for each].

For $\alpha \neq 0$, $E_{\rm int}$ depends on the orientation angle of the pair $\eta$, defined as the angle between the line joining the vortices and the in-plane polarization direction. We illustrate this in Fig. 4 for $\alpha = \pi/4$ and $\varepsilon_{\rm dd} = 5$. For the VA pair [4(a)], $E_{\rm int}$ is maximal for $\eta = \pi/2$ and decreases monotonically to 0 as $\eta \to 0, \pi$. For moderate separations $d \lesssim 6\xi_0$ (dotted red line and solid black line), the vortex ripples dominate the vortex interaction (see inset). For $\eta = 0$, the ripples from each vortex (aligned in $x$) merge side by side. As $\eta$ is increased, this side-by-side formation is broken at energetic cost. For $\eta \sim \pi/2$ one might expect, for appropriate $d$, a scenario where the inner ripples from each vortex overlap at energetic benefit. However, the intervortex density is suppressed due to the high flow velocity there (Bernoulli's principle). Beyond the ripples, $E_{\rm int}$ approaches a sinusoidal dependence on $\eta$ (dashed green line).

For the VV pair [4(b)] no such suppression occurs. As the pair is rotated, and for suitably large $d$ ($d \gtrsim 2\xi_0$), the inner ripples combine at significant energetic benefit such that $E_{\rm int}$ is minimal for $\eta = \pi/2$. At smaller separations, this overlap cannot occur and $E_{\rm int}(\eta)$ is dominated by the effect of the outer ripples (as for the VA pair), such that the $\eta = 0$ case is most energetically favored. For intermediate $d$ ($d \sim 3\xi_0$), there is energetic competition between the inner and outer ripples. At larger $d$, the modulation becomes approximately sinusoidal with $\eta$.

The effects of DDIs upon vortex pair dynamics are now considered. For $\varepsilon_{\rm dd} = 0$, VA pairs form moving solitary wave solutions for $d \gtrsim 2\xi_0$ [48]. For $d \lesssim 2\xi_0$ the cores overlap and the pair is unstable to annihilation [Fig. 5(a)]. In Fig. 1(a), we saw significant core narrowing (relative to $\xi_0$) for $\varepsilon_{\rm dd} \approx -0.4$. These conditions can stabilize the VA pair against annihilation [Fig. 5(a), red lines] [49]. For $\varepsilon_{\rm dd} = 0$ (or $\alpha = 0$), VV pairs undergo circular corotation [50] [black curve, Fig. 5(b)]. Since in-plane ($\alpha \neq 0$) DDIs cause $E_{\rm int}$ to vary as the VV pair rotates, the vortices corotate in an anisotropic path [blue and magenta curves,

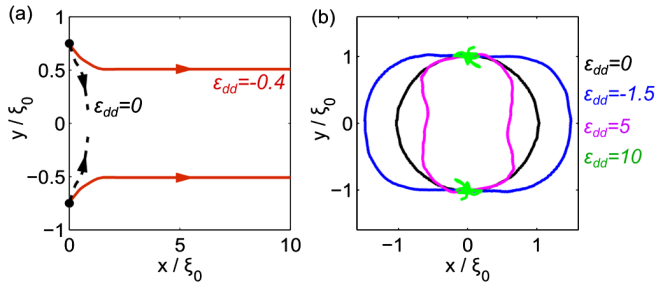


FIG. 5 (color online). (a) A VA pair (initial separation $d = 1.5\xi$) with no DDIs annihilates while DDIs ($\alpha = 0$) stabilize the pair (red lines). (b) A VV pair ($d = 2\xi_0$) with no DDIs corotates in a circular path. Off-axis ($\alpha = \pi/4$) DDIs lead to anisotropic paths and even suppression of corotation altogether.

Fig. 5(b)]. Moreover, with strong anisotropic ripples for small separations, the vortices are unable to corotate, instead "wobbling" about their initial positions [green curves, Fig. 5(b)].

We have shown that the interaction of two vortices can be significantly different in quantum ferrofluids than in conventional superfluids. At short range the vortex-vortex interaction is strongly modified by the changed shape and peripheral density ripples of each vortex. At longer range, each vortex experiences the dipolar mean-field potential of the other, with $1/\rho^2$ and $\ln(\rho)/\rho^3$ contributions. The vortex-vortex interaction is most significantly modified up to mid-range separations ($d \lesssim 10\xi$), beyond which it reduces to the usual hydrodynamic behavior. When the dipoles have a component in the plane, the vortex-vortex interaction becomes anisotropic. The vortex-vortex interaction is a pivotal building block for understanding macroscopic superfluid phenomena. For example, it is the key input parameter for models of quantum turbulence [51], the BKT transition [24], and vortex crystals [52]. The striking effects of DDIs on the dynamics of vortex pairs point to interesting new regimes for macroscopic systems of superfluid vortices.

B. C. M. acknowledges support from the Overseas Research Experience Scholarship, University of Melbourne, and D. H. J. O. acknowledges support from NSERC (Canada).

[1] R. E. Rosensweig, *Ferrohydrodynamics* (Dover Publications, New York, 1997).
[2] S. S. Hakim and J. B. Higham, Proc. Phys. Soc. London **80**, 190 (1962).
[3] M. D. Cowley and R. E. Rosensweig, J. Fluid Mech. **30**, 671 (1967).
[4] T. Lahaye, C. Menotti, L. Santos, M. Lewenstein, and T. Pfau, Rep. Prog. Phys. **72**, 126401 (2009).
[5] A. Griesmaier, J. Werner, S. Hensler, J. Stuhler, and T. Pfau, Phys. Rev. Lett. **94**, 160401 (2005).
[6] Q. Beaufils, R. Chicireanu, T. Zanon, B. Laburthe-Tolra, E. Maréchal, L. Vernac, J.-C. Keller, and O. Gorceix, Phys. Rev. A **77**, 061601(R) (2008).

[7] M. Lu, N. Q. Burdick, S. H. Youn, and B. L. Lev, Phys. Rev. Lett. **107**, 190401 (2011).

[8] K. Aikawa, A. Frisch, M. Mark, S. Baier, A. Rietzler, R. Grimm, and F. Ferlaino, Phys. Rev. Lett. **108**, 210401 (2012).

[9] T. Lahaye, T. Koch, B. Fröhlich, M. Fattori, J. Metz, A. Griesmaier, S. Giovanazzi, and T. Pfau, Nature (London) **448**, 672 (2007).

[10] T. Lahaye, J. Metz, B. Fröhlich, T. Koch, M. Meister, A. Griesmaier, T. Pfau, H. Saito, Y. Kawaguchi, and M. Ueda, Phys. Rev. Lett. **101**, 080401 (2008).

[11] N. G. Parker, C. Ticknor, A. M. Martin, and D. H. J. O'Dell, Phys. Rev. A **79**, 013617 (2009).

[12] J. L. Bohn, R. M. Wilson, and S. Ronen, Laser Phys. **19**, 547 (2009).

[13] S. Ronen, D. C. E. Bortolotti, and J. L. Bohn, Phys. Rev. Lett. **98**, 030406 (2007).

[14] D. H. J. O'Dell, S. Giovanazzi, and G. Kurizki, Phys. Rev. Lett. **90**, 110402 (2003).

[15] L. Santos, G. V. Shlyapnikov, and M. Lewenstein, Phys. Rev. Lett. **90**, 250403 (2003).

[16] A. Amo, J. Lefrère, S. Pigeon, C. Adrados, C. Ciuti, I. Carusotto, R. Houdré, E. Giacobino, and A. Bramati, Nat. Phys. **5**, 805 (2009).

[17] D. Kuchemann, J. Fluid Mech. **21**, 1 (1965).

[18] P. G. Saffman and G. R. Baker, Annu. Rev. Fluid Mech. **11**, 95 (1979).

[19] H. J. Lugt, *Vortex Flow in Nature and Technology* (John Wiley and Sons, New York, 1983).

[20] A. L. Fetter, J. Low Temp. Phys. **161**, 445 (2010).

[21] D. V. Freilich, D. M. Bianchi, A. M. Kaufman, T. K. Langin, and D. S. Hall, Science **329**, 1182 (2010).

[22] H. Aref, Annu. Rev. Fluid Mech. **15**, 345 (1983).

[23] S. Middelkamp, P. J. Torres, P. G. Kevrekidis, D. J. Frantzeskakis, R. Carretero-González, P. Schmelcher, D. V. Freilich, and D. S. Hall, Phys. Rev. A **84**, 011605 (R) (2011).

[24] Z. Hadzibabic, P. Kruger, M. Cheneau, B. Battelier, and J. Dalibard, Nature (London) **441**, 1118 (2006).

[25] S. Yi and H. Pu, Phys. Rev. A **73**, 061602(R) (2006).

[26] M. Abad, M. Guilleumas, R. Mayol, M. Pi, and D. M. Jezek, Phys. Rev. A **79**, 063622 (2009).

[27] R. M. Wilson, S. Ronen, J. L. Bohn, and H. Pu, Phys. Rev. Lett. **100**, 245302 (2008); R. M. Wilson, S. Ronen, and J. L. Bohn, Phys. Rev. A **79**, 013621 (2009).

[28] N. R. Cooper, E. H. Rezayi, and S. H. Simon, Phys. Rev. Lett. **95**, 200402 (2005); J. Zhang and H. Zhai, Phys. Rev. Lett. **95**, 200403 (2005); F. Malet, T. Kristensen, S. M. Reimann, and G. M. Kavoulakis, Phys. Rev. A **83**, 033628 (2011).

[29] K.-K. Ni, S. Ospelkaus, D. Wang, G. Quéméner, B. Neyenhuis, M. H. G. de Miranda, J. L. Bohn, J. Ye, and D. S. Jin, Nature (London) **464**, 1324 (2010).

[30] C. J. Pethick and H. Smith, *Bose-Einstein Condensation in Dilute Gases* (Cambridge University Press, Cambridge, England, 2002).

[31] T. Koch, T. Lahaye, J. Metz, B. Frölich, A. Griesmaier, and T. Pfau, Nat. Phys. **4**, 218 (2008).

[32] S. Giovanazzi, A. Görlitz, and T. Pfau, Phys. Rev. Lett. **89**, 130401 (2002).

[33] N. G. Parker and D. H. J. O'Dell, Phys. Rev. A **78**, 041601 (R) (2008).

[34] C. Ticknor, R. M. Wilson, and J. L. Bohn, Phys. Rev. Lett. **106**, 065301 (2011).

[35] Y. Cai, M. Rosenkranz, Z. Lei, and W. Bao, Phys. Rev. A **82**, 043623 (2010).

[36] U. R. Fischer, Phys. Rev. A **73**, 031602 (2006).

[37] D. H. J. O'Dell, S. Giovanazzi, and C. Eberlein, Phys. Rev. Lett. **92**, 250401 (2004).

[38] R. M. W. van Bijnen, N. G. Parker, S. J. J. M. F. Kokkelmans, A. M. Martin, and D. H. J. O'Dell, Phys. Rev. A **82**, 033612 (2010).

[39] M. Klawunn and L. Santos, Phys. Rev. A **80**, 013611 (2009).

[40] See Supplemental Material at http://link.aps.org/supplemental/10.1103/PhysRevLett.111.170402 for details of the numerical methods and calculation of the vortex-vortex interaction energy.

[41] This is our motivation for scaling length in terms of $\xi_0$.

[42] More generally the ripple wavelength and location of the first peak varies with $\varepsilon_{\rm dd}$, $\alpha$, and $\sigma$, but the latter remains within a few $\xi_0$ of the vortex origin.

[43] M. Klawunn, R. Nath, P. Pedri, and L. Santos, Phys. Rev. Lett. **100**, 240403 (2008).

[44] A. L. Fetter, in *Lectures in Theoretical Physics*, edited by K. T. Mahanthappa and W. E. Brittin (Gordon and Breach, New York, 1969).

[45] D. H. J. O'Dell and C. Eberlein, Phys. Rev. A **75**, 013604 (2007).

[46] *Handbook of Mathematical Functions with Formulas, Graphs, and Mathematical Tables*, edited by M. Abramowitz and I. A. Stegun (Dover Publications, New York, 1972).

[47] H. Wu and D. W. L. Sprung, Phys. Rev. A **49**, 4305 (1994).

[48] C. A. Jones and P. H. Roberts, J. Phys. A **15**, 2599 (1982); C. Rorai, K. R. Sreenivasan, and M. E. Fisher, arXiv:1212.6389 [Phys. Rev. B (to be published)].

[49] The initial motion of the vortices towards each other is a transient effect associated with starting the simulation with a vortex pair solution obtained in the static frame.

[50] L. M. Pismen, *Vortices in Nonlinear Fields* (Clarendon, Oxford, 1999).

[51] *Quantized Vortex Dynamics and Superfluid Turbulence*, Springer Lecture Notes in Physics Vol. 571, edited by C. F. Barenghi, R. J. Donnelly, and W. F. Vinen (Springer, Berlin, 2001).

[52] H. Aref, P. K. Newton, M. A. Stremler, T. Tokieda, and D. L. Vainchtein, Adv. Appl. Mech. **39**, 1 (2003).

Author/s:
Mulkerin, BC; van Bijnen, RMW; O'Dell, DHJ; Martin, AM; Parker, NG

Title:
Anisotropic and Long-Range Vortex Interactions in Two-Dimensional Dipolar Bose Gases

Date:
2013-10-22

Citation:
Mulkerin, B. C., van Bijnen, R. M. W., O'Dell, D. H. J., Martin, A. M. & Parker, N. G. (2013). Anisotropic and Long-Range Vortex Interactions in Two-Dimensional Dipolar Bose Gases. PHYSICAL REVIEW LETTERS, 111 (17), https://doi.org/10.1103/PhysRevLett.111.170402.

Persistent Link:
http://hdl.handle.net/11343/43018